DOI 10.1007/s11204-023-09897-w
Soil Mechanics and Foundation Engineering, Vol. 60, No. 4, September, 2023 (Russian Original No. 4, July-August, 2023)

SOIL MECHANICS

MICROSCOPIC MECHANISM OF COARSE-GRAINED SOIL UNDER TRIAXIAL TEST BASED ON PFC-FLAC COUPLING METHOD

UDC 624.131.376.5/624.131.212

X. Zhang,[1] K. Luo,[1] T. Wang,[1] M. Jiang,[1*] J. Feng,[2] and G. Mei[1]

[1]College of Civil Engineering and Architecture, Key Laboratory of Disaster Prevention and Structural Safety of Ministry of Education, Guangxi University, Nanning, Guangxi, China;
[2]College of Civil Engineering and Architecture, GuiZhou Mingzu University, Guiyang, China,
*Corresponding author E-mail: 20180121@gxu.edu.cn.

This study investigated the microscopic mechanism of coarse-grained soil under triaxial loading using the Particle Flow Code (PFC) – Fast Lagrangian Analysis of Continua (FLAC) coupling method. A numerical model considering the influence of flexible membrane deformation under triaxial loading was established according to the gradation of the material. Then, the validity and reliability of the numerical model were verified by comparison with the laboratory triaxial test results. On this basis, the motion law of particles and the change law of the force chain between the particles were analyzed from the mesoscopic perspective. The coordination number, meso-mechanism of deformation, failure (number of cracks), and energy variation during the loading process were investigated. The deformation mechanism of coarse-grained soil is explained from the mesoscopic perspective: coarse-grained soil mainly depends on a skeleton consisting of particles to bear loads. The deformation of soil is caused by the movement of particles, filling of voids, and change of the particle skeleton structure. The coordination number develops as the axial strain increases. The cracks in the model were mainly shear cracks, which is consistent with the results of the laboratory triaxial test. Finally, the loading process of the coarse-grained soil was closely related to the variation of energy.

1. Introduction

Coarse-grained soil consists of gravel and loose coarse particles with different sand and soil particle sizes. From a geotechnical perspective, coarse-grained soil has particular physical and mechanical properties, such as compactness, high water permeability, negligible deformation, and high capacity, and has been widely used as a coarse aggregate material in geotechnical engineering (slopes, earth dams, and foundation pits). However, its microscopic mechanisms under triaxial testing remain unclear. To better understand the behavior of coarse-grained soil under triaxial testing, it is important to investigate the soil's mechanical properties [1, 2].

The internal structure of coarse-grained soil is difficult to investigate owing to the typical inhomogeneity and discontinuity of the traditional Finite Element Method (FEM) [3, 4]. Moreover, the FEM faces difficulty in terms of elucidating the failure mechanism of coarse-grained soil from the mesoscopic perspective. The Particle Flow Code (PFC) method, which simulates the motion and interaction of rigid particles based on the Discrete Element Method (DEM), is more appropriate for solving the above-mentioned problems [5]. In PFC, a geotechnical material is defined as a collection of interacting particles. The basic material element of PFC can either be a rigid particle or a group of several particles bonded together to simulate particles with different shapes. The PFC has been shown to be important for understanding the complicated behavior of coarse-grained soil, such as its behavior under uniaxial compression, direct shear testing, triaxial testing, and so on. Moreover, the contact parameters of the particles in PFC are particularly important. The contact relationships for the material element of the PFC are considerably simplified compared with the block discrete elements; thus, the calculation becomes significantly more efficient.

Translated from Osnovaniya, Fundamenty i Mekhanika Gruntov, No. 4, July-August, 2023.
0038-0741/23/6004-0323

In the past decade, numerical modeling has been increasingly used for simulating the mechanical behavior of soil in geotechnical engineering. In geotechnical mechanics, the PFC is one of the most extensively used numerical methods. Backstrom et al. [6] investigated the relationship between the mesoscopic parameters of granite and the stress–strain curve using the DEM. Cho et al. [7] analyzed the influence of particle shapes on the tensile and compressive strength of rocks. To date, few studies have numerically simulated coarse-grained soil using PFC. Potyondy et al. [8] used the bonded-particle model (BPM) to simulate the important properties of rocks. Hazzard et al. [9] used BPM to simulate rocks and used the interparticle bond fracture to simulate cracks. Shao et al. [10] used PFC to investigate the triaxial test of coarse-grained soil and analyzed the influence of the meso-parameters on the test results. Deluzarche et al. [11] simulated a rockfill dam using the PFC, and analyzed the influence of the shape and friction on the stability of a rockfill dam. However, their study only considered two dimensions.

According to the literature, studies using the PFC for coarse-grained soil have mainly focused on two dimensions, and most studies have not considered the influence of flexible membrane deformation (the sleeve is a rigid wall). Moreover, the meso-mechanism of deformation and failure has not been investigated. Based on the above analysis, it is understood that PFC is a more suitable method for investigating the triaxial testing of coarse-grained soil. Hence, to investigate the meso-mechanism of coarse-grained soil under triaxial testing, this study established a three-dimensional PFC model using the PFC-FLAC coupling method, which can reflect the true deformation and failure mechanisms of coarse-grained soil. On this basis, the stress-strain curves obtained by the numerical simulation were compared to the laboratory triaxial test results. Subsequently, the meso-mechanism of the coarse-grained soil was analyzed by considering the stress–strain relationship, particle displacement, contact force chain, crack propagation, and energy change. Through the above analysis, various meaningful conclusions were drawn.

2. Numerical Model Construction and Mesoscopic Parameter Calibration

2.1. Numerical modeling using PFC-FLAC coupling method

In the FEM, the constitutive model is used to reflect the material deformation and mechanical behavior. However, PFC numerical tests can be performed to obtain the stress–strain relationship of coarse-grained soil based on the contact parameters of particles.

The created PFC walls coincide with the zone faces or shell-based structural element surfaces. In other words, the FLAC3D zones are wrapped with PFC walls. Additionally, the walls consist of edge-connected triangular faces with vertex velocities and locations. The PFC-FLAC coupling method takes the forces and moments and determines an equivalent force system on the walls. Moreover, the forces and stiffness contributions are transferred to the gridpoints [12]. This coupling method has been used in triaxial compression tests. Tan et al. [13] also used the PFC-FLAC coupling method to analyze DEM particles wrapped by a shell structure (FEM) and obtained excellent results.

The tested coarse-grained soil material was gravel from a large face rockfill dam in Dashixia [14]. The size of the soil samples was 600 mm (diameter of 300 mm) and the dry density of the soil was 2.04 g/cm^3.

Particles with a size of 5-60 mm accounted for 75% of the total weight. According to the particle gradation curve obtained by the laboratory test, the particle aggregates were consistent. To improve the computational efficiency, the minimum particle size was controlled to 5 mm in the numerical model. In fact, when the average particle size is less than 1/30 of the overall model size, the size effect can be ignored [15,16]. The specific particle gradation is shown in Fig. 1a.

The dimensions of the numerical model were determined by performing a laboratory triaxial test on the coarse-grained soil. The upper and lower loading plates were rigid walls with the same particle stiffness as the model coarse-grained soil. A sleeve that could deform laterally was created from a shell element using the FEM. The elastic modulus of the sleeve was 1e6, Poisson's ratio was 0.25, and the thickness was 0.25 m, and density ρ = 930 kg/m^3. The PFC-FLAC method was adopted between the particle and the sleeve [12]. The advantage of the PFC-FLAC coupling method is that the sleeve in FLAC can undergo large defor-

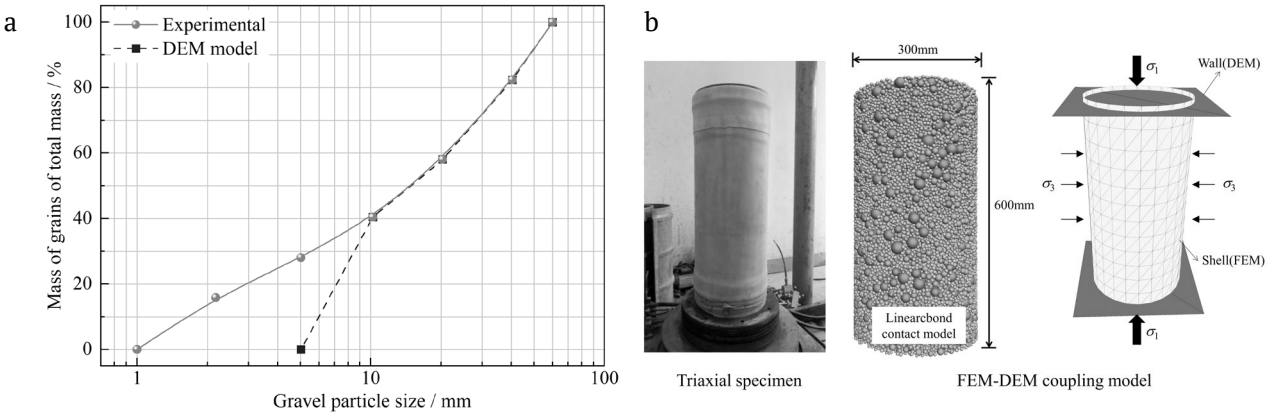

Fig. 1. Simulation of coarse-grained soils under the triaxial compression test: a) particle size distribution of coarse-grained soils, b) PFC model of coarse-grained soils.

mations compared with the rigid wall in PFC. Therefore, the results are more accurate and reliable. The PFC triaxial model is shown in Fig. 1b.

The servo control system of the triaxial compression test equipment was established by the relative motion of the upper and lower loading plates, which moved at very small speed. The stress of the sleeve was automatically adjusted using the FISH function to maintain the confining pressure. Additionally, the confining pressure was strictly controlled to less than 1% during the loading process. Finally, the loading stopped automatically when the deformation reached the strain of 20%.

2.2. Mesoscopic parameter calibration

According to the stress–strain curves obtained by the laboratory triaxial tests, a group of ideal PFC mesoscopic parameters was obtained by calibration (density of the particles is 2,530 kg/m^3, effective modulus E_c = 1.5e8 N/m , normal-to-shear stiffness ratio k_n/k_s = 1, friction coefficient μ = 0.5, normal and tangential bond strength are 1.5e5 and 5e5 Pa, respectively). To simulate the contact properties of the coarse-grained soil particles, a linear contact bond model (linearcbond) was used in this study. The linearcbond is a linear model that may be used in ball-to-ball and ball-to-facet interactions [17]. These two springs have specific tensile and shear strength [18-20].

3. Results and Analysis

3.1. Stress-strain curves

The numerical results reveal that the stress–strain relationship is in good agreement with that obtained by the laboratory tests (Fig. 2a). According to the numerical test results, the model was in the elastic stage as the axial strain increased under the initial load. As the axial strain increased further, shear planes formed owing to the internal failure of the model. When the model was in the plastic stage, the strain was approximately 11.2%, and the stress reached the maximum value (2.9 MPa). Generally, the stress–strain curves of the coarse-grained soil exhibited softening characteristics.

3.2. Displacement cloud of numerical model

Figure 2a records the particle displacement of coarse-grained soil during the loading process; A1–A4 corresponds to the three-dimensional displacement cloud of P1-P4 in the stress-strain curve, and a1–a4 corresponds to the internal particle displacement vector map of the middle section of the three-dimensional specimen of A1-A4.

It can be seen that the particles at both ends of the specimen moved toward the middle of the specimen as the strain increased. Then, the particles at the middle of the specimen were gradually squeezed outward. As the axial compression increased, the deformation at the middle of the specimen gradually increased. The deforma-

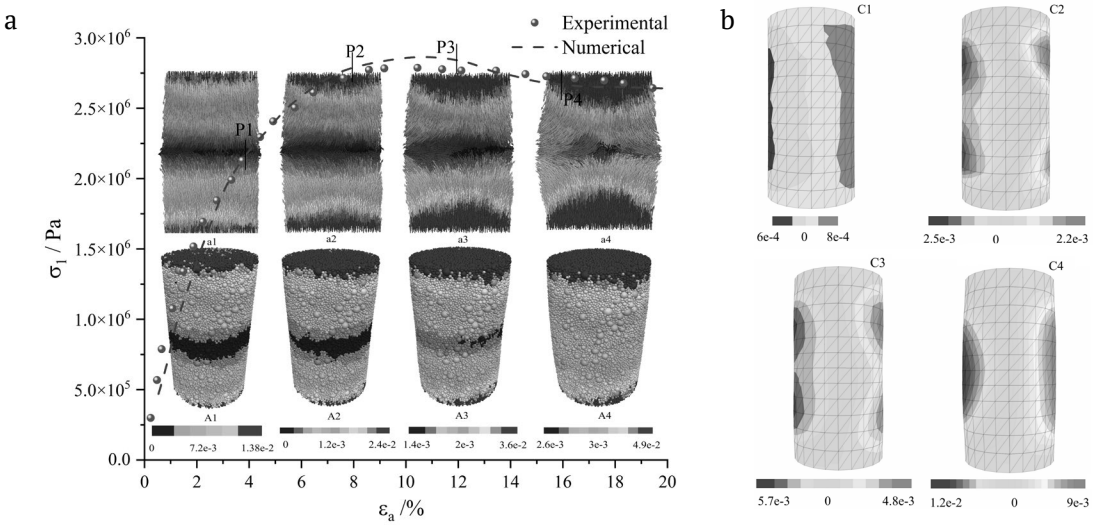

Fig. 2. Stress-strain curves and displacement cloud of the numerical model: a) particle and b) shell element.

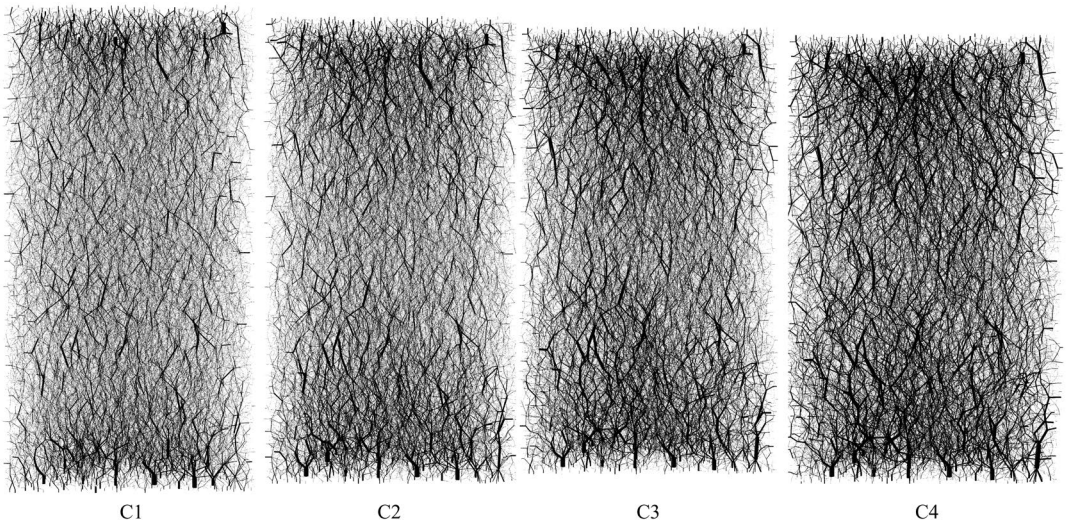

Fig. 3. Force chain distribution of samples.

tion mechanism of the coarse-grained soil can be explained from the mesoscopic perspective: coarse-grained soil mainly depends on a skeleton consisting of particles to bear the load. The deformation of soil is caused by the movement of particles, the filling of voids, and the change of the particle skeleton structure.

Figure 2b shows the displacement cloud of the shell element. As can be clearly seen, the radial displacement of the shell element gradually increased as the strain increased, and the maximum displacement of the shell element reached 9 mm. Compared with the rigid wall, the shell element reflects the true deformation and failure of coarse-grained soil.

3.3. Force chain distribution of numerical model

Figure 3 shows the samples' force chain distributions corresponding to different strains. The strength of the force chain and its changing rules can be observed: as the strain increased, the force chain gradually became denser and developed toward the middle of the sample. From a mesoscopic viewpoint, the connection between the soil particles gradually changed from a looser state to a compacted state as the confining pressure increased.

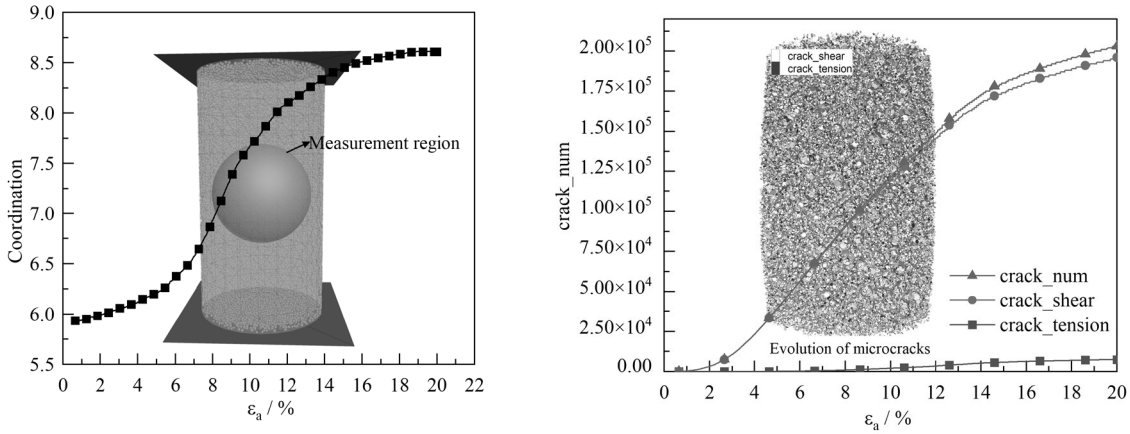

Fig. 4. Curves of coordination number (a) and cracks (b) with strain.

3.4. Analysis of coordination number changes

The coordination number (C) is the average number of contacts of the particles, and reflects the contact characteristics of coarse-grained soil from the mesoscopic perspective. A larger coordination number means that the particles in the sample are closer and the contact force between the particles is greater.

Figure 4a shows the curves of the coordination number with the strain. At the initial loading stage, the particle arrangement was relatively loose and the coordination number was small. As the load increased, the pores were filled as the particles pressed against each other. Moreover, the coordination number increased, and the intergranular bite force and shear strength were enhanced. When the load approached the maximum value, the sliding between the particles intensified and the bite force between the particles and the shear strength diminished. When the strain increased further, shear failure began to occur.

3.5. Analysis of cracks and energy

The total number of cracks (intergranular bond fractures), and the number of cracks caused by shear failure and tensile failure are plotted against the development of axial strain (Fig. 4b).

The variation trend of the number of shear cracks is essentially consistent with the total number of cracks. Moreover, the number of tensile cracks is very small. In the early stages of loading, the total number of cracks grew slowly. When the strain was greater than 3%, the total number of cracks sharply increased and then began to level off. Additionally, the cracks in the model are mainly shear cracks, which is consistent with the laboratory triaxial test results.

The dissipation and release of energy in the model are characteristics of the stress evolution of coarse-grained soil. The monitoring of the dissipation and release of energy can be realized during the loading process, and the sum of work done by the wall on the particles is defined as the boundary energy. The energy stored in the contact model between all particles is the strain energy. The energy consumed by the sliding between particles is the friction energy. Kinetic energy is the energy consumed by the movement of all particles. According to the energy conservation law, dissipative energy is defined as the boundary work minus the total strain energy [21]. The variation of energy in the stress–strain process is shown in Fig. 5. The stress–strain curve is divided into four stages, as described below.

In the initial stages of loading, all boundary work is converted into strain energy, and there is essentially no energy dissipation. With ongoing loading, the friction energy increases at a small linear rate, and the specimen exhibits linear elasticity from the macroscopic viewpoint. Moreover, the growth rate of the boundary work and strain energy gradually increases, which causes strain hardening and energy accumulation. Additionally, the dissipated energy essentially increases linearly. As the stress increases, the specimens exhibit plastic yield, and the growth rate of friction energy and the dissipated energy increase. Furthermore, both the strain energy and the boundary work increase but the rate decreases and the strain energy

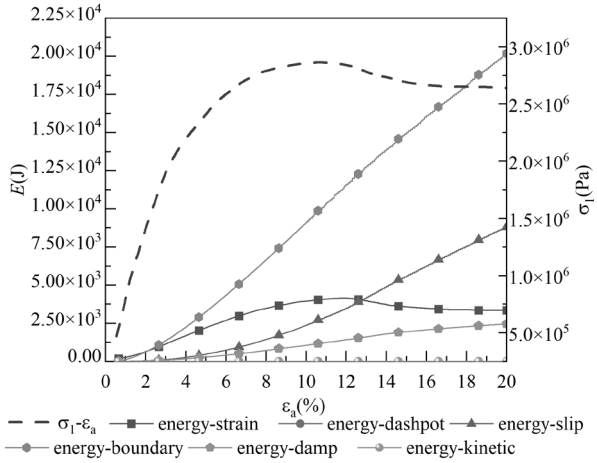

Fig. 5. Curves of energy with strain.

reaches the maximum value. The growth rate of friction energy increases owing to the increase of the relative slip between particles. Because of the rapid release of strain energy and the continuous increase of boundary work, the proportion of dissipated energy to the total energy gradually increases until the specimen fails. The proportion of kinetic energy to the total energy is very small throughout the loading stage.

Conclusions

This study used the PFC method to investigate the strength and deformation properties of coarse-grained soil. A numerical model was established according to the gradation of the material. On this basis, the validity and reliability of the numerical model were verified by comparison with laboratory triaxial test results.

The motion law of particles and the change law of the force chain between the particles were analyzed from the mesoscopic perspective. As the strain increased, the particles at both ends of the specimen moved toward the middle of the specimen, and the radial displacement of the sleeve gradually increased. Furthermore, the force chain gradually became denser and developed toward the middle of the sample. The coordination number developed with the increase in axial strain. The cracks in the model were mainly shear cracks, which is consistent with the laboratory triaxial test results. Finally, the dissipation and release of energy were recorded during the loading process. In conclusion, there is a close relationship between the macroscopic mechanical properties and the microscopic properties of coarse-grained soil.

Acknowledgments

This work was supported by the National Natural Science Foundation of China (No. 52108309, No.52008124, No.52268054 and No.52168046), by the Foundation of Guangdong Key Laboratory of Oceanic Civil Engineering (LMCE202103), the Systematic Project of Guangxi Key Laboratory of Disaster Prevention and Engineering Safety (Number 2020ZDK003), the China Postdoctoral Science Foundation (2020M683210), and the National Natural Science Foundation of Guangxi in China 2021GXNSFBA196091.

References

1. A. Bagherzadeh-Khalkhali and A. A. Mirghasemi, "Numerical and experimental direct shear tests for coarse-grained soils," *Particuology*, **7**, 83-91 (2009).
2. J. J. Wang, Y. Yang, and H. J. Chai, "Strength of a roller compacted rockfill sandstone from in-situ direct shear test," *Soil Mech. Found. Eng.*, **53**, 30-34 (2016).
3. W. Wang, P. He, and D. Zhang, "Finite element simulation based on soil meso-structures extracted from digital image," *Soil Mech. Found. Eng.*, **51**, 17-22 (2014).

4. N. Benmebarek, H. Labdi, and S. Benmebarek, "A numerical study of the active earth pressure on a rigid retaining wall for various modes of movements," *Soil Mech. Found. Eng.*, **53**, 39-45 (2016).
5. P. A. Cundall and O. D. L. Strack, "A discrete numerical model for granular assemblies," *Geotech.*, **29**, 47-65 (1979).
6. A. Bäckström, J. Antikainen, and T. Backers, et al, "Numerical modelling of uniaxial compressive failure of granite with and without saline porewater," *Int. J. Rock Mech. Min. Sci.*, **45**, 1126-1142 (2008).
7. N. Cho, C. D. Martin, and D. C. Sego, "A clumped particle model for rock," *Int. J. Rock Mech. Min. Sci.*, **44**, 997-1010 (2007).
8. D. O. Potyondy and P. A. Cundall, "A bonded-particle model for rock," *Int. J. Rock Mech. Min. Sci.*, **41**, 1329-1364 (2004).
9. J. F. Hazzard and R. P. Young, "Simulating acoustic emissions in bonded-particle models of rock," *Int. J. Rock Mech. Min. Sci.*, **37**, 867-872 (2000).
10. L. Shao, S. C. Chi, and Y. F. Jia, "Meso-mechanical simulation of a large scale triaxial test of rockfill materials," *Rock and Soil Mechanics*, **30**, 239-243 (2009).
11. R. Deluzarche and B. Cambou, "Discrete numerical modelling of rockfill dams," *Int. J. Numer. Anal. Methods Geomech.*, **30**, 1075-1096 (2006).
12. Itasca Consulting Group, 2015. Particle Flow Code in Three Dimensions: User's Manual, version 5.0, Minneapolis, USA.
13. X. Tan, Z. Hu, M. Cao, et al., "3D discrete element simulation of a geotextile-encased stone column under uniaxial compression testing," *Comput. Geotech.*, **126**, 103769 (2020).
14. M. J. Jiang, J. Zhu, S. Chen, et al., "Experimental study on the approach to predict the shear strength of in-situ sandy gravel," *Soil Mech. Found. Eng.*, **56**, 178-183 (2019).
15. H. T. Liu and X. H. Cheng, "Discrete element analysis for size effects of coarse-grained soils," *Rock and Soil Mechanics*, **30**, 287-292 (2009).
16. G. Q. Cai, S. P. Liu, J. Z. Song, et al., "Insight into relationships between macroscopic and grain-scale parameters in calculating three-dimensional discrete element of unsaturated soils," *Journal of Hunan University (Natural Sciences)*, **45**, 106-112 (2018).
17. D. O. Potyondy and P. A. Cundall, "A bonded-particle model for rock," *Int. J. Rock Mech. Min.*, **41,** 1329-1364 (2004).
18. W. Salim and B. Indraratna, "A new elastoplastic constitutive model for coarse granular aggregates incorporating particle breakage," *Can. Geotech. J.*, **41**, 657-671 (2004).
19. A. B. Kh, A. A. Mirghasemi, and S. Mohammadi, "Numerical simulation of particle breakage of angular particles using combined DEM and FEM," *Powder Technol.*, **205**, 15 (2011).
20. E. Alaei and A. Mahboubi, "A discrete model for simulating shear strength and deformation behaviour of rockfill material, considering the particle breakage phenomenon," *Granul. Matter*, **14**, 707-717 (2012).
21. J. W. Park and J. J. Song, "Numerical simulation of a direct shear test on a rock joint using a bonded-particle model," *Int. J. Rock Mech. Min. Sci.*, **46**, 1315-1328 (2009).